# Active Noise Control in Pardis Coach using Different Fuzzy Controllers

**D. Younesian, S. Hamzavi , M.R. Rostam**

1. Center of Excellence in Railway Transportation, School of Railway Engineering, Iran University of Science and Technology

*Younesian@iust.ac.ir

**Abstract**

In recent years, need to increase the convenience of trips in railway vehicles causes that train operators and manufacturers focus on reducing the noise level which is sensed by passengers. In this paper, first the state of modeling acoustic noise in cab train is discussed and natural frequencies and acoustic mode shapes are derived and then formulation of acoustic pressure in the cab will be obtained. By utilizing field testing, the noise produced by diesel engine in the cabin of Pardistranset train (source of undesirable noise), has been measured and is used in simulating. In order to reduce the acoustic pressure, a secondary noise source is used which its Stimulation signal is obtained by phased PID controller. Then, active noise control will be investigated in two cases of single-channel and multi-channel. The result of actuating the controller shows that in central frequencies of one octave band, there is a reduction in the sound pressure level, loudness, and sound loudness level.

***Keywords**: passive noise control, active noise control, acoustic pressure, phased PID controller*

## 1. Introduction

The World Health Organization introduces noise as the most obvious health damage of working people. This issue is known as the environmental noise pollution and can effect on body health [1].

In recent years, need to increase the convenience of trips in railway vehicles causes that train operators and manufacturers focus on reducing the noise level which is sensed by passengers. By using modern equipment’s for the mechanism of noise reduction, there will be a significant decrease in sound pressure level of the cabin which finally, reaches the convenience of passengers to a desirable level [2].

Noise control is carried out in two major methods. Passive noise control is used for noise reduction at high frequencies. At low frequencies, sound Insulators and absorbers in large dimensions is needed because the acoustic wavelength is large. But, considering that available space is one of the design limiter factors, it is necessary to use another method for noise reduction [3]. Because of this reason, the technology of active noise control is used in order to reduce noise in low frequencies. Active noise control which is a modern technology in the field of undesirable noise reduction, includes producing a sound field electro-acoustically (usually with loudspeakers) in order to eliminate the undesirable noise field. Active noise control is an industry purpose because it cost less than passive noise control for controlling the noises with low frequencies. Although the passive noise control is expensive and not convenience and at most cases is not possible because of high acoustic waves [4], modern active sound control systems include one or more sources of control which apply a secondary distribution to the system. This distribution neutralizes the undesirable sound which is produced by one or more primary sources [5]. The range of performance of these two methods is shown in figure 1 [6].

The most important feature of modern active noise control systems is their adaptively so they can be adapted by minor changes in the system which should be controlled. These changes include cases like change in temperature and relative humidity of acoustic environment and depreciation produced in source of control (loudspeaker). There only needs minor changes to neutralize the un adaptive control system [7]. The acoustic processes have nonlinear characteristics based on actuators features and the nature of the Phenomenon itself. Recent researches confirm the importance of nonlinear controllers which cause increase in the efficiency of this type of systems [9, 8, 2, 10].

## 2. Formulation

### 2.1 The acoustic modal analysis of rectangular cavity

In order to calculating the acoustic pressure into the train cabin, it is assumed like a rectangular cavity. Based on this assumption the equation of acoustic wave for 3D rectangular cavity is given as [11]

$$\nabla^2 P - \frac{1}{c^2}\frac{\partial^2 P}{\partial t^2} = 0 \tag{1}$$

where $P$ is acoustic pressure and $c$ is the speed of sound. The Eq. (1) can be rewritten in the Cartesian coordinate as follow

$$\frac{\partial^2 P}{\partial x^2} + \frac{\partial^2 P}{\partial y^2} + \frac{\partial^2 P}{\partial z^2} - \frac{1}{c^2}\frac{\partial^2 P}{\partial t^2} = 0 \tag{2}$$

In order to modal analysis and obtaining the natural frequencies and the acoustic mode shapes the separation of variables procedure is used. Thus, the acoustic pressure in the rectangular cavity is consider as

$$P(x,y,z,t) = \psi(x,y,z)q(t) \tag{3}$$

where $q(t)$ is the function of time and the modal function $\psi(x,y,z)$ can be separated as follow

$$\psi(x,y,z) = X(x)Y(y)Z(z) \tag{4}$$

by substituting Eq. (3) and Eq. (4) into the Eq. (2) and after some manipulation Eq. (2) is reduced to

$$c^2\left(\frac{X''}{X} + \frac{Y''}{Y} + \frac{Z''}{Z}\right) = \frac{\ddot{q}}{q} = cte = -\omega^2 \tag{5}$$

where $\omega$ is the constant number and Eq. (5) can be rewritten as

$$\frac{X''}{X} + \frac{Y''}{Y} + \frac{Z''}{Z} = -\frac{\omega^2}{c^2} = -K^2 = -(K_x^2 + K_y^2 + K_z^2) \tag{6}$$

after of separating of Eq. (6) the following equations are obtained

$$\frac{X''}{X} = -K_x^2 \Rightarrow X(x) = C\sin(K_x x) + D\cos(K_x x) \tag{7}$$

$$\frac{Y''}{Y} = -K_y^2 \Rightarrow Y(y) = C^*\sin(K_y y) + D^*\cos(K_y y) \tag{8}$$

$$\frac{Z''}{Z} = -K_z^2 \Rightarrow Z(z) = C^{**}\sin(K_z z) + D^{**}\cos(K_z z) \tag{9}$$

in which $K_x$, $K_y$, $K_z$, $C$, $C^*$, and $C^{**}$ are unknown constants that are found later by imposing the boundary conditions. Considering the rigid and non-absorbent walledrectangular cavity as shown in Fig. 2.

the boundary conditions are obtained from Eq. (10) through Eq. (12) as follow

$$\begin{cases} x = 0 \\ x = L_x \end{cases} \Rightarrow \frac{\partial P}{\partial x} = 0 \Rightarrow \frac{\partial X}{\partial x} = 0 \tag{10}$$

$$\begin{cases} y = 0 \\ y = L_y \end{cases} \Rightarrow \frac{\partial P}{\partial y} = 0 \Rightarrow \frac{\partial Y}{\partial y} = 0 \tag{11}$$

$$\begin{cases} z = 0 \\ z = L_z \end{cases} \Rightarrow \frac{\partial P}{\partial z} = 0 \Rightarrow \frac{\partial Z}{\partial z} = 0 \tag{12}$$

then, the unknown constants of Eqs(7-9) are found as given in the following equations

$$C = C^* = C^{**} = 0 \tag{13}$$

$$\begin{cases} K_x = \dfrac{r\pi}{L_x}, & r = 0,1,2,... \\ K_y = \dfrac{m\pi}{L_y}, & m = 0,1,2,... \\ K_z = \dfrac{n\pi}{L_z}, & n = 0,1,2,... \end{cases} \tag{14}$$

Finally, the $rmn$ *th* natural frequencies of rectangular cavity are obtained as

$$\omega_{rmn} = cK = c\sqrt{\left(\frac{r\pi}{L_x}\right)^2 + \left(\frac{m\pi}{L_y}\right)^2 + \left(\frac{n\pi}{L_z}\right)^2} \tag{15}$$

And the $rmn$ th modal function or acoustic modes are found as

$$\psi_{rmn}(x,y,z) = \cos\left(\frac{r\pi}{L_x}x\right)\cos\left(\frac{m\pi}{L_y}y\right)\cos\left(\frac{n\pi}{L_z}z\right) \tag{16}$$

### 2.2 Calculating the internal acoustic pressure of cavity with noise source

The source noises in the cavity are considered such as the forced term in the acoustic wave equation. For example, for the mono pole source (loud speaker), the mass flow rate is given [12]

$$\dot{m}(x,y,z,t) = \rho Q(x,y,z,t) \tag{17}$$

where $\dot{m}$, $Q$, $\rho$ are the mass flow rate, the volume flow rate and the density of the acoustic medium, respectively. Therefore, the wave equation rewritten as

$$\nabla^2 P - \frac{1}{c^2}\frac{\partial^2 P}{\partial t^2} = -\frac{\rho\dot{Q}}{V} \tag{18}$$

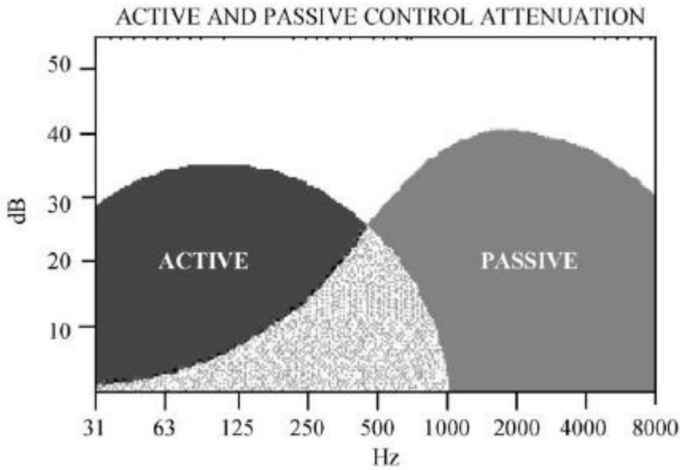


**Fig1.** The effective range of performance for active and passive noise control

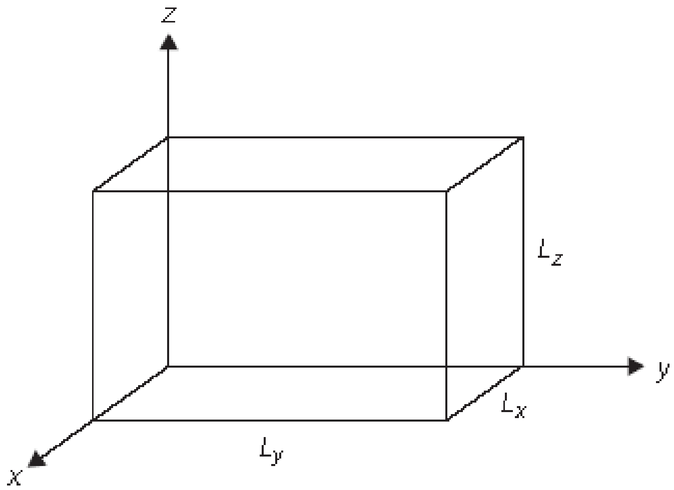


**Fig2.** The rectangular cavity.

in which $\dot{Q}$ is the partial derivative of the volume flow rate respect to the time and $V$ is the volume of the cavity. The volume flow rate of the source can be written as the product of the location of the source and the function of the time as follow

$$Q(x,y,z,t) = Q(t)V\delta(x-x_0)\delta(y-y_0)\delta(z-z_0) \quad (19)$$

where $\delta$ is the Dirac delta function and $(x_0, y_0, z_0)$ is the location of the source.In order to simplifying the equations, replacing the subscript $n$ instead of the subscripts $r, m, n$ in the equations (15) and (16). Then, the natural frequencies of the cavity are arranged according to increasing the value of the natural frequencies and shown with the subscript $n$. Based on the Galerkin method or the Eigen function expansion the solution of the Eq. (18) can be obtained as follow

$$P(x,y,z,t) = \sum_{n=0}^{\infty} P_n(t)\psi_n(x,y,z) \quad (20)$$

where $P_n(t)$ is the time-dependent function. Substituting Eq. (20) into Eq. (18) then multiplying both sides of Eq. (18) by $\psi_m$ and integrating over the volume of the cavity yields to

$$\sum_{n=0}^{\infty} p_n(t)\int_V \psi_m \nabla^2 \psi_n dV - \frac{1}{c^2}\sum_{n=0}^{\infty} \ddot{p}_n(t)\int_V \psi_m \psi_n dV = -\rho\dot{Q}\int_V \psi_m \delta(x-x_0)\delta(y-y_0)\delta(z-z_0)dV \quad (21)$$

The orthogonally relation between the acoustic mode shapes expressed as

$$\int_V \psi_n \psi_m dV = \begin{cases} 0 & m \neq n \\ V_n & m = n \end{cases} \quad (22)$$

By substituting the Eq. (22) into Eq. (21) and after some manipulations one obtained

$$\ddot{P}_n(t) + \omega_n^2 P_n(t) = \frac{\rho c^2 \psi_n(x_0, y_0, z_0)}{V_n}\dot{Q} \quad (23)$$

Solving the differential Eq. (23) gives the time-dependent function $P_n(t)$ corresponding to the $n$ th mode and finally used the Eq. (20) for calculating the acoustic pressure in the specific point $(x, y, z)$. Note that Eq. (23) is obtained for the cavity with non-absorbent wall. The equation for the cavity with rigid and absorbent wall is given as

$$\ddot{P}_n(t) + 2\zeta_n\omega_n\dot{P}_n(t) + \omega_n^2 P_n(t) = \frac{\rho c^2 \psi_n(x_0, y_0, z_0)}{V_n}\dot{Q} \quad (24)$$

where $\zeta_n$ is the critical damping ratio corresponding to the $n$ th mode.

### 2.3Fuzzy PID controller design

In order to adapt to changing environmental conditions, the controller should has be adaptive. Since the most of the industrial controller used the PID plan and also have benefits such as robust performance and general applicability for most of the systems [13,14], in this section consider the adaptive property of the PID controller that gains of controller are obtained by using the fuzzy systems. The transfer function of the PID controller given as

$$G(s) = k_p + \frac{k_i}{s} + k_d s \quad (25)$$

where $k_p$, $k_i$, $k_d$ are the property, integral and derivative gains, respectively. Another equivalent expression for PID controller is

$$u(t) = k_p\left[e(t) + \frac{1}{T_i}\int_0^t e(\tau)d\tau + T_d\dot{e}(t)\right] \quad (26)$$

Where $T_i = k_p/k_i$ the integral time is constant, $T_d = k_d/k_p$ is the derivative time constant, $u(t)$ is the control signal, $e(t)$ is the error signal and $\dot{e}(t)$ is the derivative of error signal respect to the time. In this section, the proposed method by Zhao, Tomizuka and Isaka will be used. Supposed to $k_p$ and $k_d$ located within the intervals $\left[k_{p,\min}, k_{p,\max}\right]$ and $\left[k_{d,\min}, k_{d,\max}\right]$. In order to simplifying the equations by using the following linear transformation, $k_p$ and $k_d$ are normalized and located within the interval $[0,1]$

$$k_p' = \frac{k_p - k_{p,\min}}{k_{p,\max} - k_{p,\min}} \quad (27)$$

$$k_d' = \frac{k_d - k_{d,\min}}{k_{d,\max} - k_{d,\min}} \quad (28)$$

Supposed to the integral and derivative time constant relations are given as follow

$$T_i = \alpha T_d \quad (29)$$

by using the Eq. (29) the following equation can be obtained

$$k_i = \frac{k_p}{\alpha T_d} = \frac{k_p^2}{\alpha k_d} \quad (30)$$

therefore, $k_p'$, $k_d'$ and $\alpha$ are parameters that found by using the fuzzy system. If these parameters can be determined, in this case the gains of PID can be obtained from the Eq. (27), Eq. (28) and Eq. (30)..

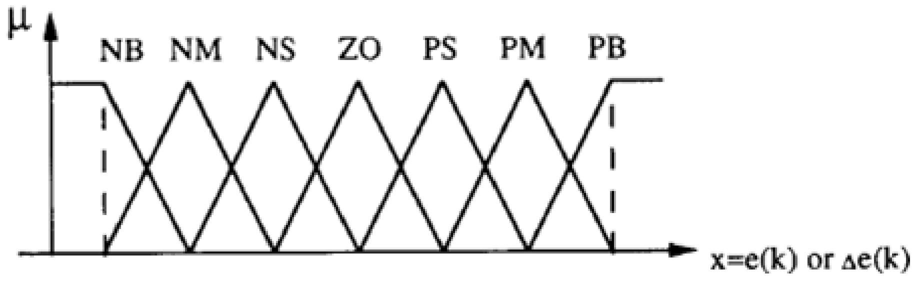


**Fig3.** The attachment function for $e(t)$ and $\dot{e}(t)$.

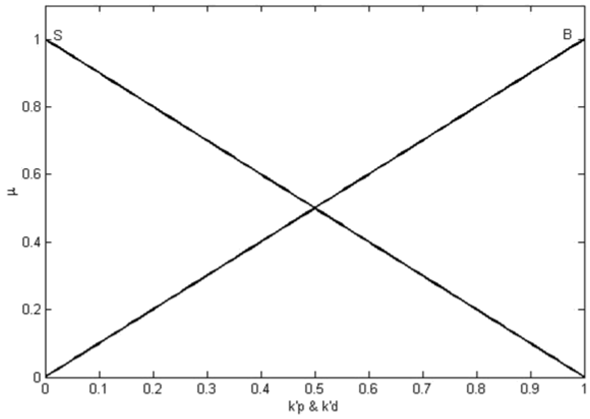


**Fig4.** The attachment functions for $k'_p$ and $k'_d$.

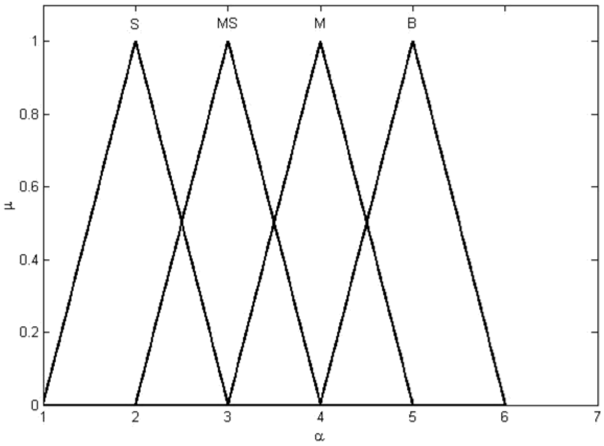


**Fig5.** The attachment functions for $k'_p$ and $k'_d$

Furthermore, the attachment functions for $k'_p$, $k'_d$ and $\alpha$ shown in Figs. 4 & 5.

Three set of fuzzy rules for determining the $k'_p$, $k'_d$ and $\alpha$, in which each set has 49 rules are shown in Tables 1-3 [15, 16].

The inputs of fuzzy system are $e(t)$ and $\dot{e}(t)$. Supposed to the domain for $e(t)$ and $\dot{e}(t)$ are $\left[e_M^-, e_M^+\right]$ and $\left[e_{Md}^-, e_{Md}^+\right]$ respectively and seven fuzzy set defined as Fig. 3 that cover the desire domain.

Furthermore, the attachment functions for $k'_p$, $k'_d$ and $\alpha$ shown in Figs. 4 & 5.

Three set of fuzzy rules for determining the $k'_p$, $k'_d$ and $\alpha$, in which each set has 49 rules are shown in Tables 1-3 [15, 16].

Finally, 49 rules in each set are combined and therefore the parameters $k'_p$, $k'_d$ and $\alpha$ are obtained according to the following equations

$$k'_p(t) = \frac{\sum_{l=1}^{49} \bar{y}_p^l \, \mu_{A^l}(e(t)) \, \mu_{B^l}(\dot{e}(t))}{\sum_{l=1}^{49} \mu_{A^l}(e(t)) \, \mu_{B^l}(\dot{e}(t))} \tag{31}$$

$$k'_d(t) = \frac{\sum_{l=1}^{49} \bar{y}_d^l \, \mu_{A^l}(e(t)) \, \mu_{B^l}(\dot{e}(t))}{\sum_{l=1}^{49} \mu_{A^l}(e(t)) \, \mu_{B^l}(\dot{e}(t))} \tag{32}$$

$$\alpha(t) = \frac{\sum_{l=1}^{49} \bar{y}_\alpha^l \, \mu_{A^l}(e(t)) \, \mu_{B^l}(\dot{e}(t))}{\sum_{l=1}^{49} \mu_{A^l}(e(t)) \, \mu_{B^l}(\dot{e}(t))} \tag{33}$$

Where $A^l$ and $B^l$ are shown in Fig. 3.

**Table. 1.** The fuzzy rules for tuning $k'_p$ .

| | | $\dot{e}(t)$ | | | | | | |
|---|---|---|---|---|---|---|---|---|
| | | NB | NM | NS | ZO | PS | PM | PB |
| $e(t)$ | NB | B | B | B | B | B | B | B |
| | NM | S | B | B | B | B | B | S |
| | NS | S | S | B | B | B | S | S |
| | ZO | S | S | S | B | S | S | S |
| | PS | S | S | B | B | B | S | S |
| | PM | S | B | B | B | B | B | S |
| | PB | B | B | B | B | B | B | B |

**Table. 2.** The fuzzy rules for tuning $k'_d$ .

| | | $\dot{e}(t)$ | | | | | | |
|---|---|---|---|---|---|---|---|---|
| | | NB | NM | NS | ZO | PS | PM | PB |
| $e(t)$ | NB | S | S | S | S | S | S | S |
| | NM | B | B | S | S | S | B | B |
| | NS | B | B | B | S | B | B | B |
| | ZO | B | B | B | B | B | B | B |
| | PS | B | B | B | S | B | B | B |
| | PM | B | B | S | S | S | B | B |
| | PB | S | S | S | S | S | S | S |

**Table. 3.** The fuzzy rules for tuning $\alpha$ .

| | | $\dot{e}(t)$ | | | | | | |
|---|---|---|---|---|---|---|---|---|
| | | NB | NM | NS | ZO | PS | PM | PB |
| $e(t)$ | NB | 2 | 2 | 2 | 2 | 2 | 2 | 2 |
| | NM | 3 | 3 | 2 | 2 | 2 | 3 | 3 |
| | NS | 4 | 3 | 3 | 2 | 3 | 3 | 4 |
| | ZO | 5 | 4 | 3 | 3 | 3 | 4 | 5 |
| | PS | 4 | 3 | 3 | 2 | 3 | 3 | 4 |
| | PM | 3 | 3 | 2 | 2 | 2 | 3 | 3 |
| | PB | 2 | 2 | 2 | 2 | 2 | 2 | 2 |

### 2.4Noise measurement of diesel engine of Pardis train

The experimental setup that selected is wagan A of transet Pardis train as shown in Fig. 6&7. Test equipment was included a microphone and notebook. The microphone attached in the wagon floor opposite of the diesel engine and by using the Spectra Lab software the time history of the acoustic pressure with sampling rate 44100 Hz (in which cover the range of human hearing) are measured as shown in Fig. 8.


**Fig6.** Wagon A of Pardis transet train.

**Fig7.** Location of diesel engine

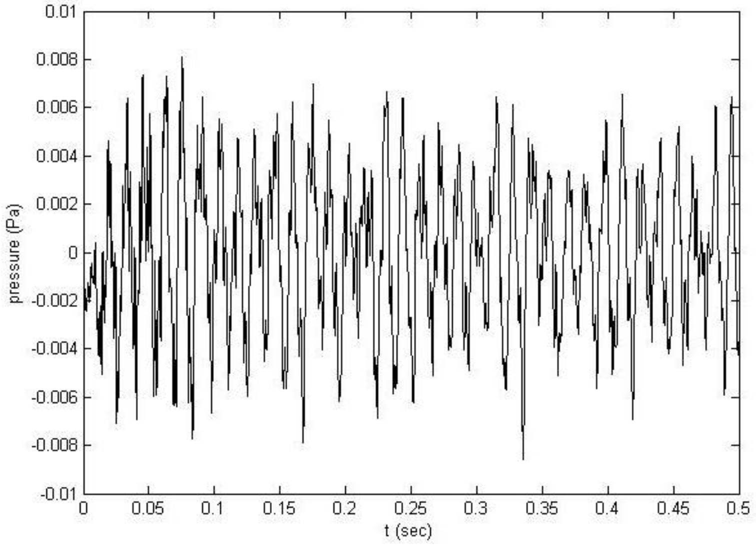


**Fig8.** The measured noise of diesel engine

**Table. 4.** System physical specification

| Row | Quantity | Unit | Value |
|---|---|---|---|
| 1 | Cavity dimension (height, width, length) | m | (17, 3, 2.5) |
| 2 | Location of noise source (height, width, length) | m | (8.8, 1.5, 0) |
| 3 | Location of passenger 1 (height, width, length) | m | (8.5, 1, 1.24) |
| 4 | Location of passenger 2 (height, width, length) | m | (9.58, 0.5, 1.24) |
| 5 | Location of loudspeaker control (height, width, length) | m | (0, 3, 2.5) |
| 6 | Critical damping ratio (ζ) | - | 0.5 |
| 7 | Sound velocity (c) | m/s | 340 |
| 8 | Air density (ρ) | kg/m$^3$ | 1.22 |

### 2.5 Simulation and results

The aim in the simulations were performed is decreasing the sound pressure level at the frequency range that less than 200 Hz. The geometric properties of system are given in Table. 4.

The result of applying the fuzzy PID controller in two cases, single-channel (control the sound pressure level at a point by one controller) for passenger 1 and multi-channel (control the sound pressure level at two points by one controller) for passengers 1 and 2 are shown in the next section.

#### 2.5.1 Single-channel

The range of errors and changes for active noise control at the location of passenger 1 are given as follow

$$e \in [-0.009\,,\,0.009] \quad \& \quad \dot{e} \in [-3\,,\,3] \qquad (34)$$

The range of proportional and derivative gains of controller expressed as

$$k_p \in [67.5\,,\,270] \quad \& \quad k_d \in [0.27\,,\,1.8] \qquad (35)$$

Fig. 9 shows the required volume acceleration for secondary noise source.

Fig. 10 displays the acoustic pressure with and without controller. It is clear that the acoustic pressure is reduced when the controller is applied. Moreover, sound pressure level in the frequencies domain that shown in Fig. 11 indicates the acoustic pressure level is decreased.

The average reduction of sound pressure level is obtained according to following equation

$$NR = 10\log\left(\frac{1}{3}(10^{\frac{8.15}{10}} + 10^{\frac{8.05}{10}} + 10^{\frac{7.9}{10}})\right) = 8.0345\ dB$$

Where $NR(dB)$ is the average reduction of sound pressure level.

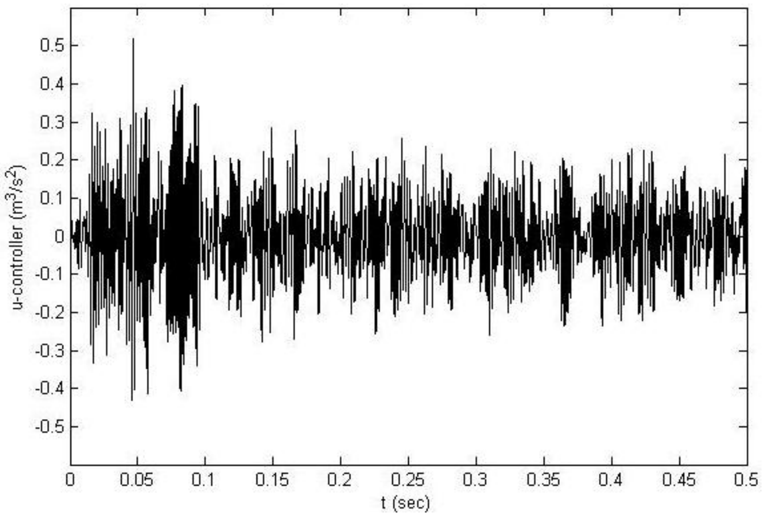


**Fig9.** The volume acceleration of loudspeaker control.

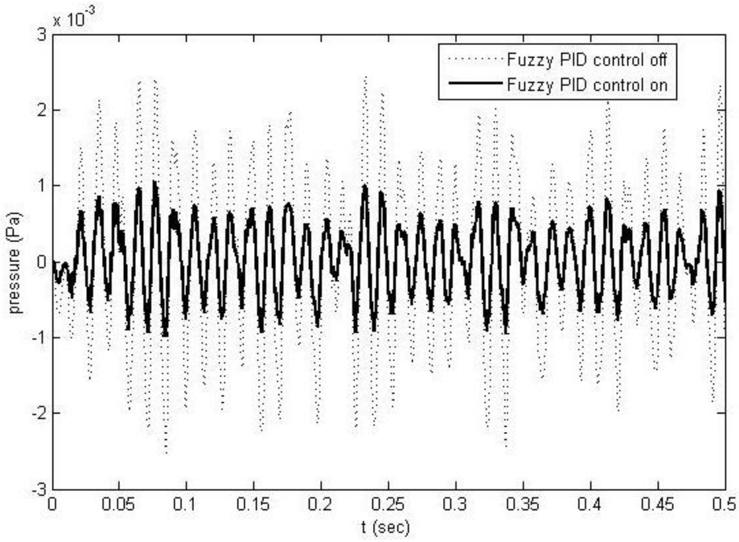


**Fig10.** The acoustic pressure in the wagon for passenger 1 with and without controller.

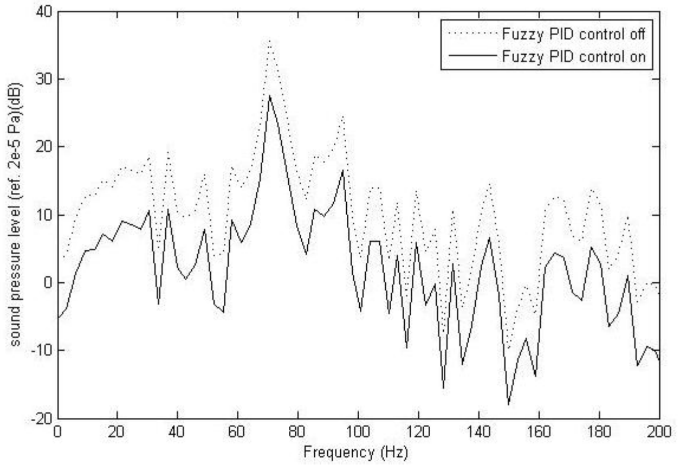


**Fig11.** Sound pressure level in the wagon for passenger 1 with and without controller.

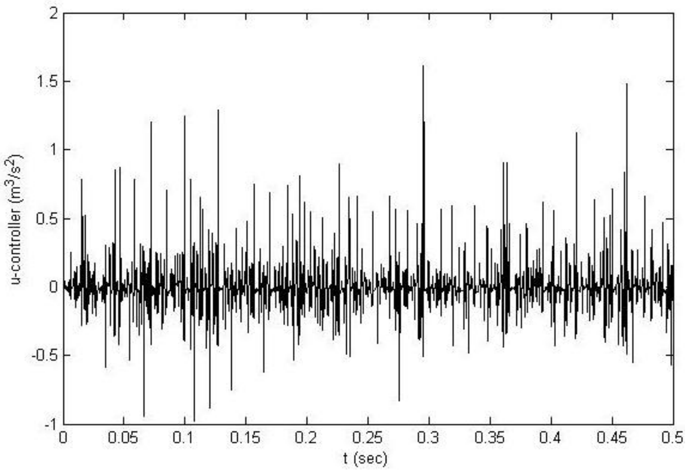


**Fig12.** The volume acceleration of loudspeaker control.

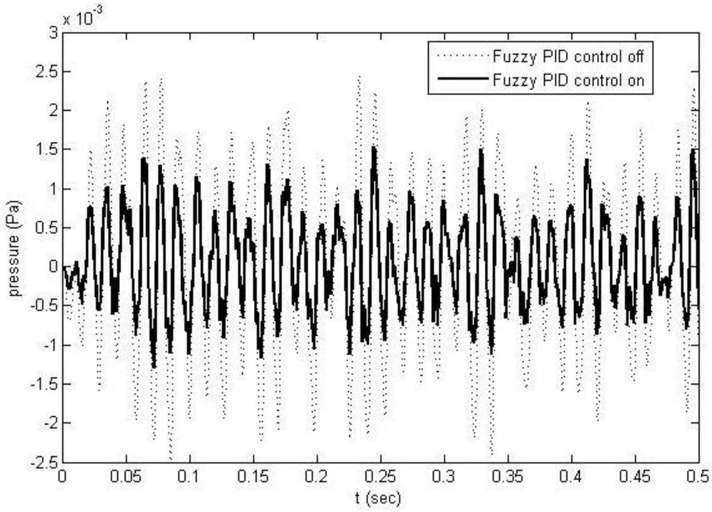


**Fig13.** The acoustic pressure in the wagon for passenger 1 with and without controller

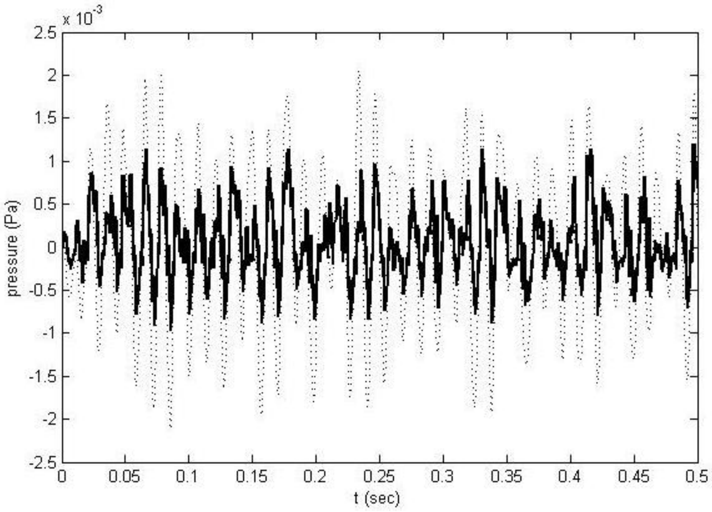


**Fig14.** The acoustic pressure in the wagon for passenger 2 with and without controller

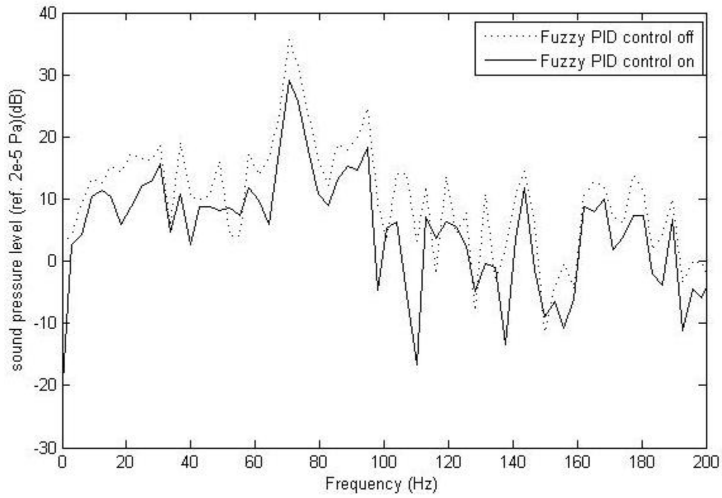


**Fig15.** Sound pressure level in the wagon for passenger 1 with and without controller.

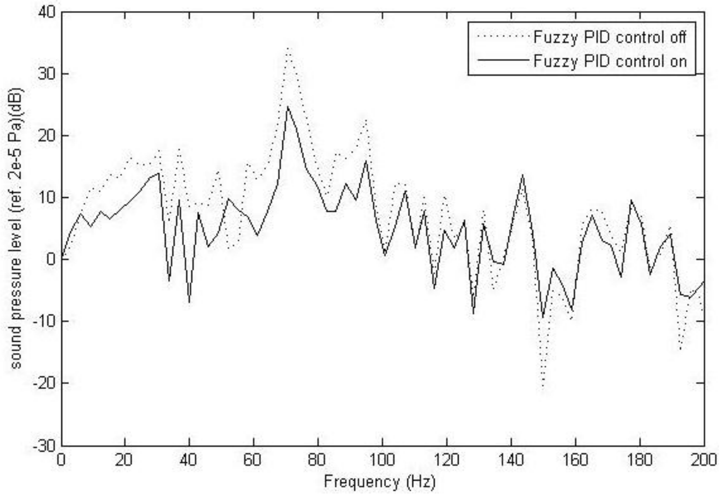


**Fig16.** Sound pressure level in the wagon for passenger 2 with and without controller.

The average reduction of sound pressure level is obtained according to following equation

$$NR = 10\log\left(\frac{1}{3}(10^{\frac{8.15}{10}} + 10^{\frac{8.05}{10}} + 10^{\frac{7.9}{10}})\right) = 8.0345\ dB$$

Where $NR(dB)$ is the average reduction of sound pressure level

### 2.5.1 Multi-channel

The aim of this section is active noise control at two points into the wagon train by using the secondary noise source which is known as multi-channel mode. The point coordinates are given in Table. 4. The ranges of error and change for both points are given as follow

$$e \in [-0.09\,,\,0.09] \quad \& \quad \dot{e} \in [-9\,,\,9] \qquad (36)$$

The ranges of proportional and derivative gains of controller for both points are obtained from Eq. (35). Fig. 12 shows the required volume acceleration for secondary noise source. Figs. 13 & 14 display the acoustic pressure with and without the controller for point 1 and 2, respectively. In addition, the sound pressure level in the frequency domain for both points is shown in Figs. 15 & 16, respectively.

In the multi-channel case, at points 1 and 2, at some time acoustic pressure further decreased than other time. This fact causes to the sound pressure level that obtained in multi-channel case for point 1 is different from the single-channel case. As can be seen in the single-channel case the more noise reduction is achieved. For point 2 as is clear from Fig. 16, sound pressure level is decreased at some frequencies range and at other ranges remains constant. The Average reduction of sound pressure level for point 1 is 5.7 dB and for point 2 is 5.6 dB.

## 3. Conclusion

The average reduction of sound pressure level for passenger 1 in the single-channel case is 8 dB (shows the satisfying results) while in the multi-channel case is 5.7 dB. Thus, the reduction of sound pressure level in multi-channel signal case is less than single-channel.

## References

[1]. Colin Hansen, noise control from concept to application, Taylor & Francis, 2005.

[2]. M.A. Botto, J.M.C. Sousa, and J.M.G.S. Costa, "Intelligent active noise control applied to a laboratory railway coach model", Control Engineering Practice 13, 2005, pp. 473-484.

[3]. S.J. Elliott and P.L. Nelson, "active noise control", IEEE signal processing magazine, 1993, pp. 12-35.

[4]. C.H. Hansen, Understanding Active Noise Cancellation, Spon Press, 2003.

[5]. S.M. Kuo, and D.R. Morgan, "Active Noise Control: A Tutorial Review", PROCEEDINGS OF THE IEEE, Vol. 87, No. 6, 1999, pp. 943-973.

[6]. J. Landaluze, I. Portilla, J.M. Pagalday, A. Martinez and R. Reyero, "application of active noise control to an elevator cabin", control engineering practice 11, 2003, pp. 1423-1431.

[7]. D.A. Bies and C.H. Hansen, Engineering Noise Control, Spon Press, 2009.

[8]. J.M. Sousa, C.A. Cilva, and J.M.G.S. Costa, "Fuzzy active noise modeling and control", International Journal of Approximate Reasoning 33, 2003, pp. 51-70.

[9]. C.A. Cilva,J.M. Sousa and J.M.G.S. Costa, "Active Noise Control Based on Fuzzy Models", 4th European Conference on Noise Control, 2001, pp. 1-14.

[10]. J. Sousa, C.A. Silva, J.M.G. S Costa, "Fuzzy active noise modeling and control of enclosures", Proceedings of 15th World Congress of the International Federation of Automatic Control, 2002, pp. 1–6.

[11]. S. Mohamady, R. K. R. Ahmad, A. Montazeri, R. Zahari3, N. Aswan and A. Jalil, "Modelling and Eigenfrequency Analysis of Sound-StructureInteraction in a Rectangular Enclosure with Finite ElementMethod", Submitted to the Journal of Advances in Acoustics and Vibration, 2009.

[12]. I.L. Ver and L.L. Beranek, Noise and Vibration Control Engineering, John Wiley & Sons, 2006.

[13]. L. Wang, A Course in Fuzzy Systems and Control, Prentice-Hall International, 1997.

[14]. Z. Zhao, M. Tomizuka and S. Isaka, "Fuzzy Gain Scheduling of PID Controllers", IEEE Transactions on Systems, MAN and Cybernetics, Vol. 23, No. 5, 1993, pp. 1392-1398.

[15]. S. Chiu and S. Pong, "In-Line Viscosity Control in an Extrusion Process With A Fuzzy Gain Scheduled PID Controller", journal of applied polymer science, Vol. 74, 1999, pp. 541-555.